Oxidation study of Pt-Al based coatings on γ-TiAl at 950°C

Authors: A. Ebach-Stahl[1], M. Fröhlich[2]

[1]DLR – German Aerospace Center, Institute of Materials Research, 51170 Cologne, Germany

[2]Leibniz Institute for Plasma Science and Technology (INP), 17489 Greifswald, Germany

Contact Information:

Corresponding author:

Andrea Ebach-Stahl

DLR – German Aerospace Center

Institute of Materials Research

Linder Höhe

51170 Cologne, Germany

Email: andrea.ebach@dlr.de

Phone: +49 (0) 2203 601 2557

Maik Fröhlich:

Leibniz Institute for Plasma Science and Technology (INP)

Felix-Hausdorff-Str. 2

17489 Greifswald, Germany

Email: maik.froehlich@inp-greifswald.de

Phone: +49 (0) 3834 554 3900

Abstract

In the present study, Pt-based aluminide coatings were deposited on γ-TiAl (Ti-45Al-8Nb-0,2C; at.%) by magnetron sputtering and tested under high temperature conditions. The Pt-content in the layer was varied (40, 50 and 100 at.%) to find an optimized oxidation resistant coating. The Pt-50Al coating showed the best oxidation resistance at 950°C due to the formation of a continuous thin alumina layer on top compared to the fast oxidizing pure Pt and aluminum rich Pt-60Al coatings.

Depending on the testing time different Pt-Ti-Al phases were formed below the grown oxide layer which is caused by the outward diffusion of Ti and the inward diffusion of Pt at the interface between coating and base material, respectively.

Beside mass gain measurements microstructural examinations were performed via scanning electron microscopy (SEM), energy-dispersive X-Ray spectroscopy (EDS) as well as X-Ray diffractometry (XRD) to study the evolution of phase formation.

Keywords: PtAl; γ-TiAl; oxidation; coating; magnetron sputtering

Introduction

In aero engines and gas turbines many different materials are applied. Whereas in the first stages of the engine the protection against erosion is interesting [1,2], the materials in the afterwards stages like compressor, combustion chamber and turbine are exposed to high temperatures, oxidation and corrosion. State of the art is the use of Ni-based superalloys as material for turbine blades regarding the high temperature resistance and attractive mechanical properties. Coatings can further extend the oxidation resistance of the components. Well engineered are coating systems like MCrAlY (M=Ni and/or Co) [3-5] or Pt-modified aluminides as oxidation protection in the hot parts of aero engines and gas turbines [6-8]. These types of coatings are alumina formers and protect the substrate due to the very slow and controlled oxide formation.

But lightweight materials come to the fore of industry interests to replace the heavy nickel base superalloys or titanium alloys. Titanium aluminides are attractive as a new material for engine components of the high pressure compressor and low pressure turbine due to their good mechanical properties in a temperature range from 700°C up to 850°C [9-10], whereas a sufficient creep resistance can be provide up to 750°C [11]. But due to the insufficient oxidation resistance at temperatures above 750°C caused by the formation of fast growing titania [12-14], it is necessary to protect the material with oxidation resistant coatings. Halogen-, TiAl-, TiAlCr- as well as Si-based coatings are examples forming a slow growing alumina layer [15-20] or thermodynamically stable phases with low oxidation rates [21-23].

According to their high oxidation resistance on Ni based superalloys Pt-aluminide coatings were tested on titanium alloys with a positive effect on the oxidation behavior [24-26]. In this work coatings with different Pt-contents were deposited on the lightweight material γ-TiAl by magnetron sputtering and tested at 950°C in air.

Experimental

Disc shaped specimens were machined from extruded γ-TiAl rods (provided by GfE, Germany, Ti-45Al-8Nb-0,8C, all compositions are given in at.%,). Their dimensions are 15 mm diameter and 1 mm thickness. Before the specimens were coated, the surface was ground with SiC paper, polished with a SiO_2 suspension and in a last step cleaned with ethanol.

Three coatings with various Pt-Al compositions with a thickness of 10µm were deposited via magnetron sputtering to study which Pt-content will provide the best oxidation resistance: pure Pt, Pt-50Al and Pt-60Al. The pure Pt was deposited using one magnetron source. The other coatings were applied with a two source equipment (Pt + Al). During the deposition process the samples rotated to ensure a homogeneous coating composition and thickness. The coating systems were tested by a cyclic exposure at 950°C in air. One cycle consists of 60 min heating time and 10 min cooling down to 60°C. The samples were pulled into the hot furnace. The heating rate is about 300°C/min. After defined exposure times (10, 100, and 1000 cycles) a sample was removed to study the microstructure evolution, respectively. If a sample showed great lateral spallation about 20% of the surface, the sample was taken out of testing procedure and declared as failure.

Mass gain measurements were recorded cyclically of all coating systems. Microstructural examinations of the coatings and the thermally grown oxide scales were performed using scanning electron microscopy (SEM), energy-dispersive X-ray spectroscopy (EDS) and X-ray diffraction (XRD). The scanning electron microscope (Leo, *Gemini DSM 982*) was operated at 3 kV in secondary electron mode. EDS analyses were carried out at an operation voltage of 20 kV using an Oxford Si detector. Chemical compositions were determined by semi-quantitative analysis (Oxford INCA software). Phase analysis was carried out by XRD using a Siemens D5000 powder diffractometer in Bragg-Brentano configuration with Cu Kα

radiation. Texture measurements were executed with a Bruker D8 Discover diffractometer using a 2D-detector.

Results and discussion

As in literature reported in detail, PtAl coatings on titanium alloys show good oxidation behavior [24-26]. To study the potential of Pt-modified aluminide coatings on γ-TiAl, two different Pt-containing aluminide coatings, Pt-50Al and Pt-60Al, as well as a pure Pt coating were investigated.

As shown in figure 1 the pure Pt coated sample shows the highest mass change and had to be taken out of testing after 140 cycles due to great lateral blistering with spallation. The Pt-50Al and Pt-60Al coatings were tested until 1000 cycles without failure, respectively. The Pt-50Al coating clearly reveals the lowest mass gain compared to the system with the highest aluminum content (Pt-60Al; see figure 1).

As SEM micrograph shows (figure 2a) most of the pure Pt coating has disintegrated due to interdiffusion and various thick oxides containing layers have formed already after 10 cycles. A mixed oxide scale consisting of Al_2O_3 and TiO_2 was formed pointed out by the increased mass gain, as shown in figure 1 and clearly visible in Fig. 2a. Several layers have formed after the short high temperature exposure: a top layer consisting of Pt + mixed oxides of TiO_2 and Al_2O_3, an intermediate layer of TiO_2 and Al_2O_3, and a metallic zone that mainly contains Ti-Pt-Al. Between this oxidation zone and intermetallic area a mixed zone presumably containing TiO_2 and or Al_2O_3 with Ti-Pt-Al was formed. A phase composition could not identify, because the phases were thinner than the spot size of SEM. For identification TEM (transmission electron microscopy) analyses would be necessary. The increasing volume of the oxides as well as enhanced oxidation at the grain boundaries may cause the spreading on top of the coating.

Investigations of Dong et al. [27] refer to a high dissociation rate of oxygen at Pt-surfaces. Due to the high concentration of oxygen ions, an enhanced oxygen transport can take place through the Pt coating. This finally leads to the inner oxidation of aluminum and titanium at the substrate/coating interface. Caused by interdiffusion between substrate and coating a niobium containing Ti-Pt-Al phase was formed. Regarding the chemical composition, shown in table 1, the phase could not identify. Also in our literature studies this phase or similar phase was not found [25, 28-30]. The chemical composition of this Ti-Pt-Al zone varies. Reasons of this dispersion could be on the one hand small not identifiable phases in this area (grew and white small isles, also shown in figure 2a), and presumably the testing-time after 10 cycles was not enough to get phase formations completely. Therefore the composition of the area varies due to partial interdiffusion. Moreover, an interdiffusion zone between coating and substrate based on the γ-TiAl phase with a slight Pt enrichment of 1-2 at.% occurred.

As shown in figure 2b, the Pt-60Al coating formed a thin alumina layer on top after 10 cycles at 950°C. Because of outward diffusion of titanium and niobium, and inward diffusion of Pt, the initially amorphous Pt-60Al coating changed into a porous layer containing $(Pt,Ti,Nb)_2Al_3$ and Al_2O_3 on top. Underneath the original coating a dense and continuous layer of the $(Pt,Ti,Nb)_2Al_3$ phase of a thickness of about 8µm has formed. Moreover, pores were formed mainly in the upper part of the coating already within 10 cycles, presumably caused by volume changes during phase formation, observable by the increased film thickness of 23 µm compared to 10 µm before exposure.

An alumina layer was also formed on top of the Pt-50Al-coated system after 10 cycles (see figure 2c). Beneath the thin thermally grown oxide the phases Pt_2Al_3, $(Ti,Nb)PtAl_2$ and (Ti,Nb)PtAl were formed (see table 1), caused by interdiffusion between γ-TiAl substrate and Pt-50Al coating. Presumably, the Pt_2Al_3 as well as $(Ti,Nb)PtAl_2$ layer are a result of Pt-depletion in the surface region. Platinum diffused inwards and combined with outward

diffusion of titanium and niobium the (Ti,Nb)$PtAl_2$ and (Ti,Nb)PtAl phases were formed. Compared to the pure Pt coating a Pt-enriched γ-TiAl zone was also observed between coating and substrate. All mentioned phases were verified by XRD-measurements (see figure 3) that are given here exemplarily for the Pt-50Al coating.

The coating evolution after 100 cycles (see figure 4) shows only slightly differences compared to the 10 cycles state. The mixed oxide scale on the Pt coated sample increased up to a thickness of about 40µm after 100 cycles (see figure 4a). The areas of titania and alumina were grown rapidly while the Pt islands became smaller. Further on, the niobium containing Ti-Pt-Al phase in the interdiffusion zone oxidized completely.

As expected the number of pores in the Pt-60Al coating increased within 100 1h-cycles (see figure 4b). Additionally, an internal oxidation process within the diffusion layer that contained substantial amounts of Pt started already. Due to further interdiffusion phase transformation took place. The titanium and niobium containing Pt_2Al_3 phase, being the only metallic one after 10 cycles, is only present in the upper part of the coating after further 90 cycles. Beneath that phase $TiPtAl_2$ and (Ti,Nb)$PtAl_2$ were formed due to the proceeded interdiffusion process between coating and substrate.

The further exposure of the Pt-50Al coated sample revealed the disappearance of the (Ti,Nb)PtAl phase accompanied by an increase of the Pt-Al based layer thickness from 20 µm (10 cycles) to 25 µm (100 cycles). The increased formation of the (Ti,Nb)$PtAl_2$ phase after 100 cycles, as shown in figure 4c, can be explained by an enhanced inward diffusion of platinum leading to the formation of phases with a higher Al content, (Ti,Nb)$PtAl_2$ and Pt_2Al_3, in the coating. Although it is not visible in the SEM-micrograph (figure 4c), the Pt_2Al_3 phase exists in the upper part of the coating. It is approved by EDS and XRD analysis. In figure 4c the grown columnar microstructure of the coating based on the magnetron sputter deposition

process and intensified by enhanced ion etching during the preparation procedure can be clearly seen.

All chemical compositions of the phases present after 100 cycles are listed in table 1.

The exposure tests revealed a failure of the Pt coated γ-TiAl sample after 140 cycles going along with blistering and spallation. Nevertheless, single Pt particles and a non-continuous platinum layer are observable in the oxidized coating, as similarly found after 100 cycles.

The Pt-60Al layer was also completely oxidized, however, after 1000 cycles. Similar to the oxidized Pt coated sample platinum particles could also be observed in the oxide scale (see figure 5a). Due to interdiffusion and Al consumption, caused by alumina formation, a small region of α_2-Ti_3Al with approximately 3 at.% Pt and Nb, respectively, was formed at the substrate/coating interface.

In contrast, the Pt-50Al coated material still shows a thin and dense thermally grown alumina scale after 1000 cycles exposure time at 950°C (see figure 5b). Due to further inward diffusion of Pt and outward diffusion of Ti and Nb the coating mainly consists of the intermetallic (Ti,Nb)$PtAl_2$ phase beneath the oxide layer with slightly different compositions compared to the shorter exposure times (see table 1). Instead of the continuous Pt_2Al_3 layer, as observed after 10 cycles, only fragments are present remaining directly beneath the alumina layer. The XRD-spectra show the oxidation and phase transformation processes in the Pt-50Al coating which took place until 10, 100 and 1000 cycles (figure 3). The intensity of the Al_2O_3 peaks increased while that of Pt_2Al_3 disappeared for longer testing time. Also the reflexes of $PtAl_2$ as well as of τ_2-$TiPtAl_2$ become more distinct with higher number of test cycles. The increasing quantity of reflexes after 1000 cycles is presumably caused by the formation of an additional phase. Probably, the continuing Nb outward diffusion could be the reason for that.

Unfortunately, a distinct phase could not be identified with the JCPDS data base. Texture effects that may have overlaid the phase identification could be excluded by texture measurements.

According to the EDS and XRD measurements the (Ti,Nb)$PtAl_2$ phase was only formed during the exposure of the Pt-50Al coating. That implies that this phase enhances the formation of alumina, ideally of a close and dense layer, resulting in an excellent oxidation resistance. Generally, the face centered intermetallic phase was stable concerning interdiffusion. (Ti,Nb)$PtAl_2$ could be observed after 10 as well as 1000 exposure cycles at 950°C looking at the Pt-50Al coated sample. The enhanced Al_2O_3 formation and, therewith, excellent oxidation resistance could be explained by the remarkable higher aluminum content of c_{Al} = 45 – 51 at.% compared to titanium c_{Ti} = 17 – 30 at.%.

Summary

Three Pt modified aluminide coatings with different Pt contents were deposited successfully on γ-TiAl by magnetron sputtering: pure Pt, Pt-50Al and Pt-60Al. The cyclic oxidation test at 950°C showed that the Pt-50Al coating exhibited the best oxidation behavior by forming a thin and dense Al_2O_3 scale while the pure Pt coated sample failed after short time. Further on, the Pt-60Al coating oxidized much faster.

The Pt-50Al coated sample is distinguished by the presence of the stable (Ti,Nb)$PtAl_2$ phase, apparently enhancing the Al_2O_3 formation due to the higher Al content compared to that of Ti. The capability of the Pt-50Al coating has to be proved by further investigations at different temperatures.

Acknowledgment

We thank J. Brien and D. Peters (German Aerospace Center, Institute of Materials Research) for the technical support and coating manufacturing and Alexander Francke for performing texture measurements.

References

[1] A. Feuerstein, A. Kleyman: Surf. Coat. Technol. 204 (2009), pp. 1092–1096

[2] W. Tabakoff: Wear 233–235, 1999, pp. 200–208

[3] B. Pint, I. Wright, W. Lee, Y. Zhang, K. Prüßner, K. Alexander, Mat.. Sci. Eng. A 245 (1998) 201–211.

[4] U. Schulz, O. Bernardi, A. Ebach-Stahl, R. Vaßen, D. Sebold: Surf. Coat. Technol., 203 (2008) 160-170

[5] U. Schulz, M. Menzebach, C. Leyens, Y. Yang: Surf. Coat. Technol. 146–147 (2001) 117–123.

[6] B. Saint-Ramond, M. Carlin, M. Silva, J.R. Nickolls: Materials Science Forum 461-464, 2004, pp. 265-272

[7] M.R. Brickey, J.L. Lee: Oxid. Met. 54, 2000, pp. 237-254

[8] J. Angenete, K. Stiller: Oxid. Met. 60, 2003, pp. 83-101

[9] H. Clemens, F. Appel, A. Bartels, H. Baur, R. Gerling, V. Güther and K. Kestler: Ti-2003, Science and Technology, Volume IV, G. Lütjering and J Albrecht, Eds.; (Wiley-VCH Verlag, Weinheim, 2004) pp. 2123-2136.

[10] H. Kestler and H. Clemens: Titanium and Titanium alloys, M. Peters and C. Leyens, Eds., (Wiley-VCH Verlag, Weinheim, 2002) pp. 369-400.

[11] H. Clemens, S. Mayer: Adv. Eng. Mat. 15 No. 4 (2013), pp. 191

[12] W. Smarsly, H. Baur, G. Glitz, H. Clemens, T. Khan and M. Thomas: Structural Intermetallics 2001, K.J. Hemker et Al., Eds., (The Minerals, Metals & Materials Society, Warrendale, 2001) pp. 25-34.

[13] M.P. Brady, W.J. Brindley, J.L. Smialek and I.E. Locci: JOM 48 (1996), pp. 46-50.

[14] M. Schmitz-Niederau, M. Schütze: Oxid. Met. 52 (1999), pp. 225-240.

[15] A. Donchev, R. Braun, M. Schütze: JOM 2010, pp. 70-74

[16] A. Donchev, B. Gleeson, M. Schütze: Intermetallics 11 (2003), pp. 387–398

[17] V. Gauthier, F. Dettenwanger, M. Schütze, V. Shemet, W.J. Quadakkers: Oxid. Met. 59, 2003, pp. 233-255

[18] Z. Liu, G. Wang: Mat. Sci. Eng. A 397, 2005, pp. 50-57

[19] C. Zhou, Y. Yang, S. Gong, H. Xu: Mat. Sci. Eng. A 307 (2001) 182-187

[20] M. Fröhlich, R. Braun, C. Leyens: Surf. Coat. Technol. 201 (2006) 3911-3917

[21] A. Ebach-Stahl, M. Fröhlich, R. Braun, C. Leyens: Adv. Eng. Mat., 2008, 10, No. 7, Wiley-VCH Verlag Weinheim, pp. 675-677

[22] Hua-Ping Xiong, Mei Mao, Yong-Hui Xie, Yao-Yong Cheng, Xiao-Hong Li: Mat. Sci. Eng. A 391 (2005), pp. 10-18

[23] X.Y. Li, S. Taniguchi, Y. Matsunaga, K. Nakagawa, K. Fujita: Intermetallics 11 (2003), pp. 143-150

[24] D.K. Das, Z. Alam: Surf. Coat. Technol. 201 (2006), pp. 3406-3414.

[25] D.K. Das, S.P. Trivedi: Mat. Sci. Eng. A 367 (2004), pp. 225-233.

[26] I. Gurappa, A.K. Gogia: Surf. Coat. Technol. 139 (2001), pp. 216-221.

[27] Q. Dong, G. Hultquist, G.I. Sproule, M.J. Graham: Corr. Sci. 49, 2007, pp. 3348-3360

[28] S.P. Trivedi, D.K. Das: Intermetallics 13, 2005, pp. 1122-1133

[29] V. Raghavan: J. Phase Equilib. Diff. 26, 2005, pp.188-189

[30] J.J. Ding, P. Rogl, B. Chevalier, J. Etourneau: Intermetallics 8, 2000, pp. 1377-1384

Figure captions

Figure 1: Mass gain of Pt-, Pt-50Al- and Pt-60Al-coated γ-TiAl at 950°C

Figure 2: SEM micrographs after 10 cycles at 950°C

a) Pt coating
b) Pt-60Al coating
c) Pt-50Al coating

Figure 3: XRD-Spectra of Pt-50Al coated samples after 10, 100 and 1000 cycles at 950°C

Figure 4: SEM micrographs after 100 cycles at 950°C

a) Pt coating
b) Pt-60Al coating
c) Pt-50Al coating

Figure 5: SEM micrographs after 1000 cycles at 950°C

a) Pt-60Al coating
b) Pt-50Al coating

Figure 1

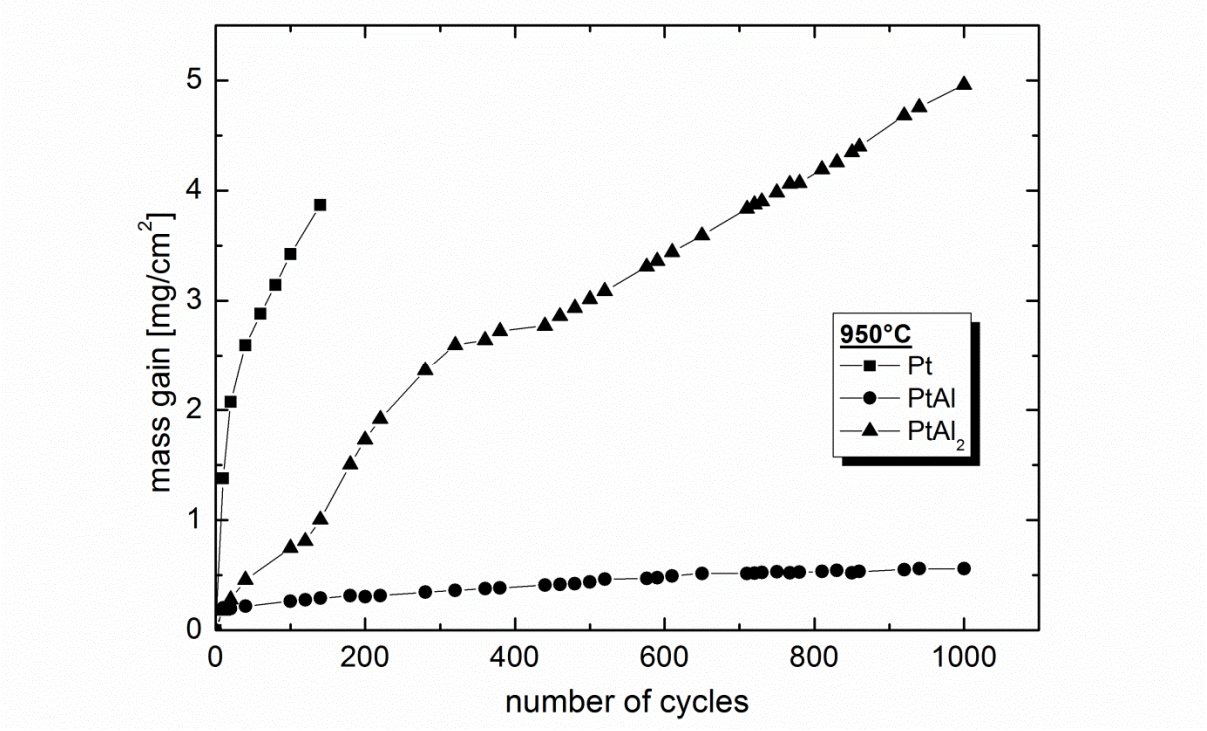

Figure 2a

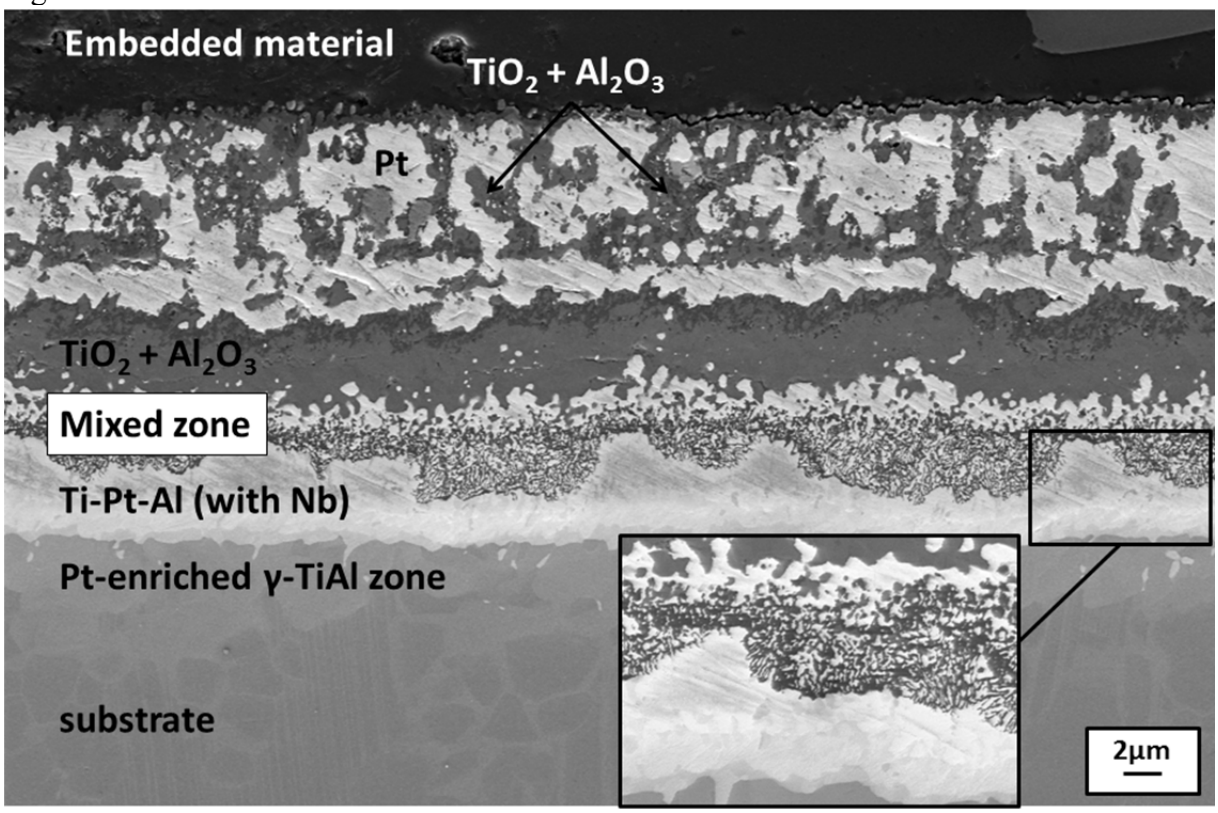

Figure 2b

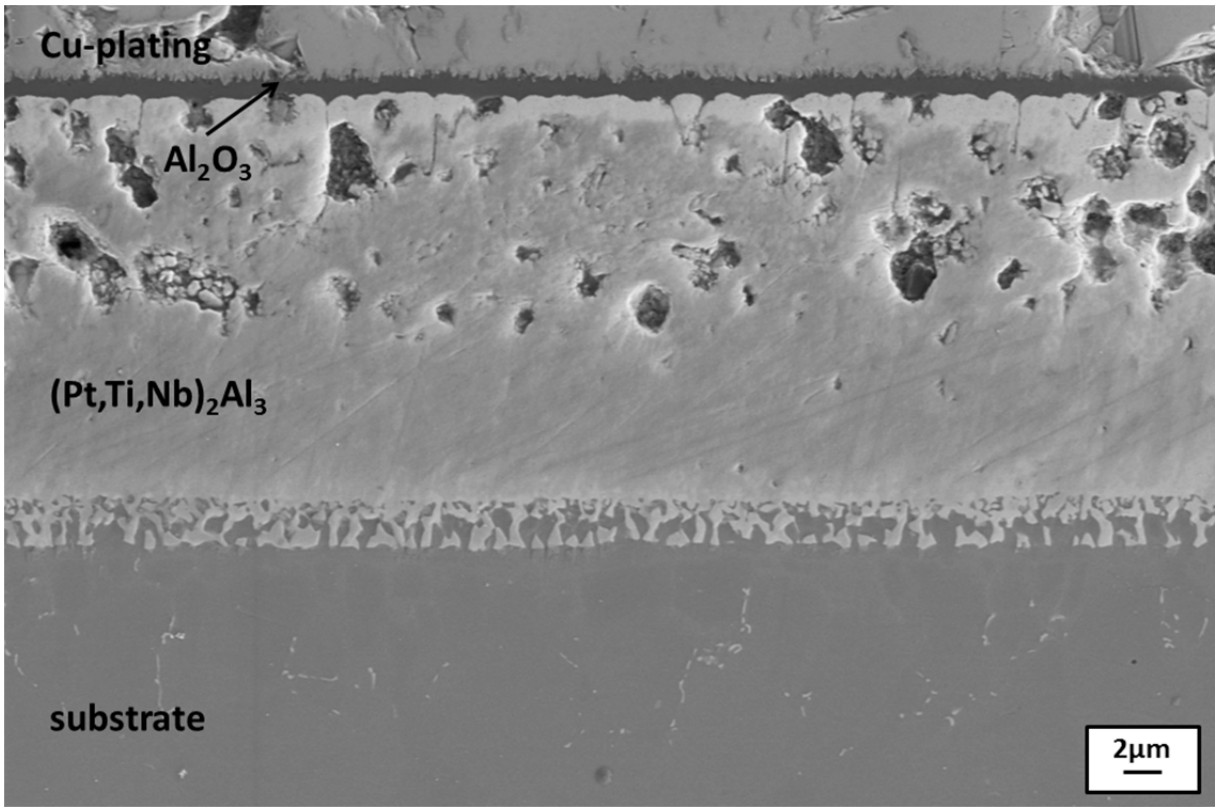

Figure 2c

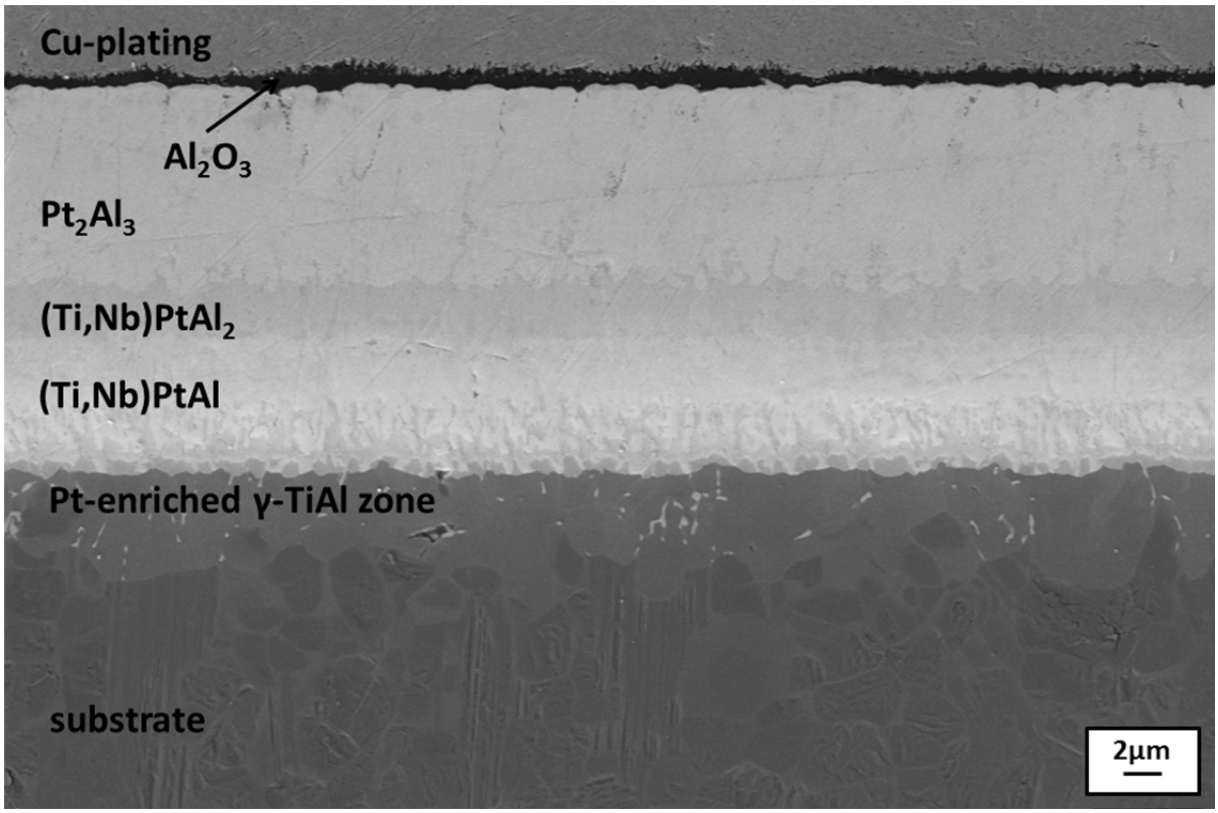

Figure 3

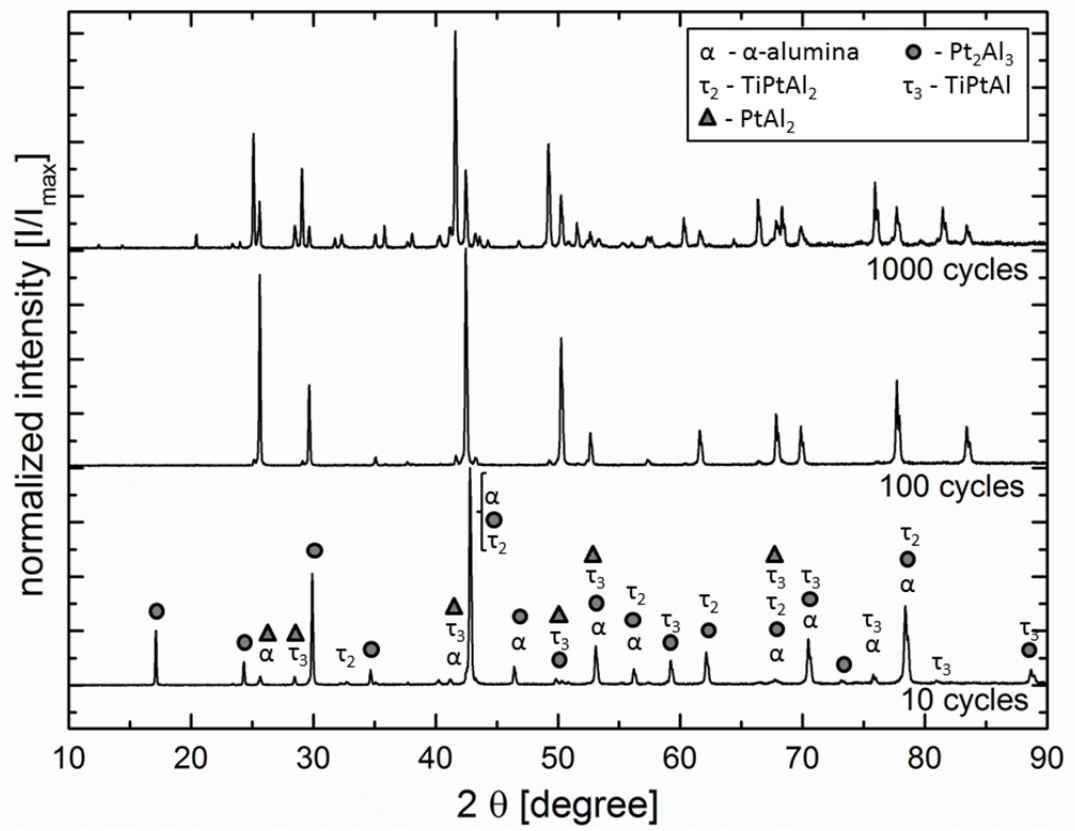

Figure 4a

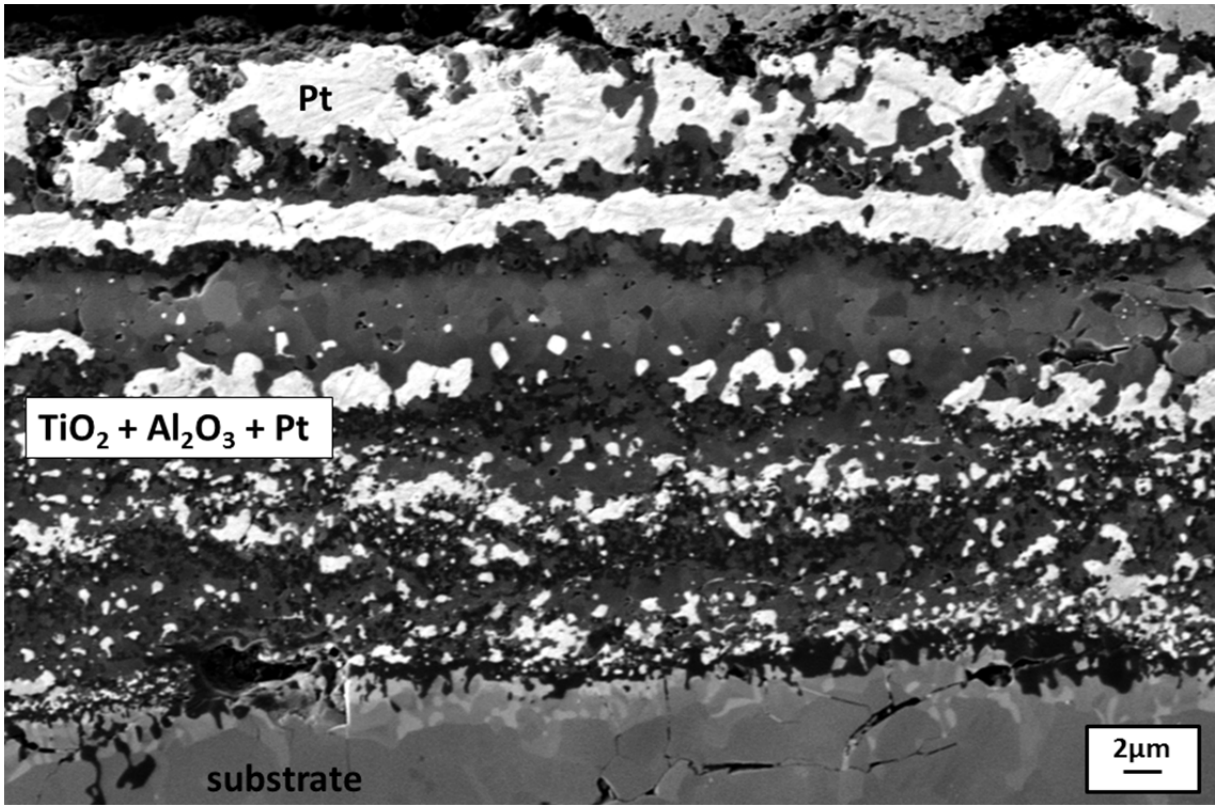

Figure 4b

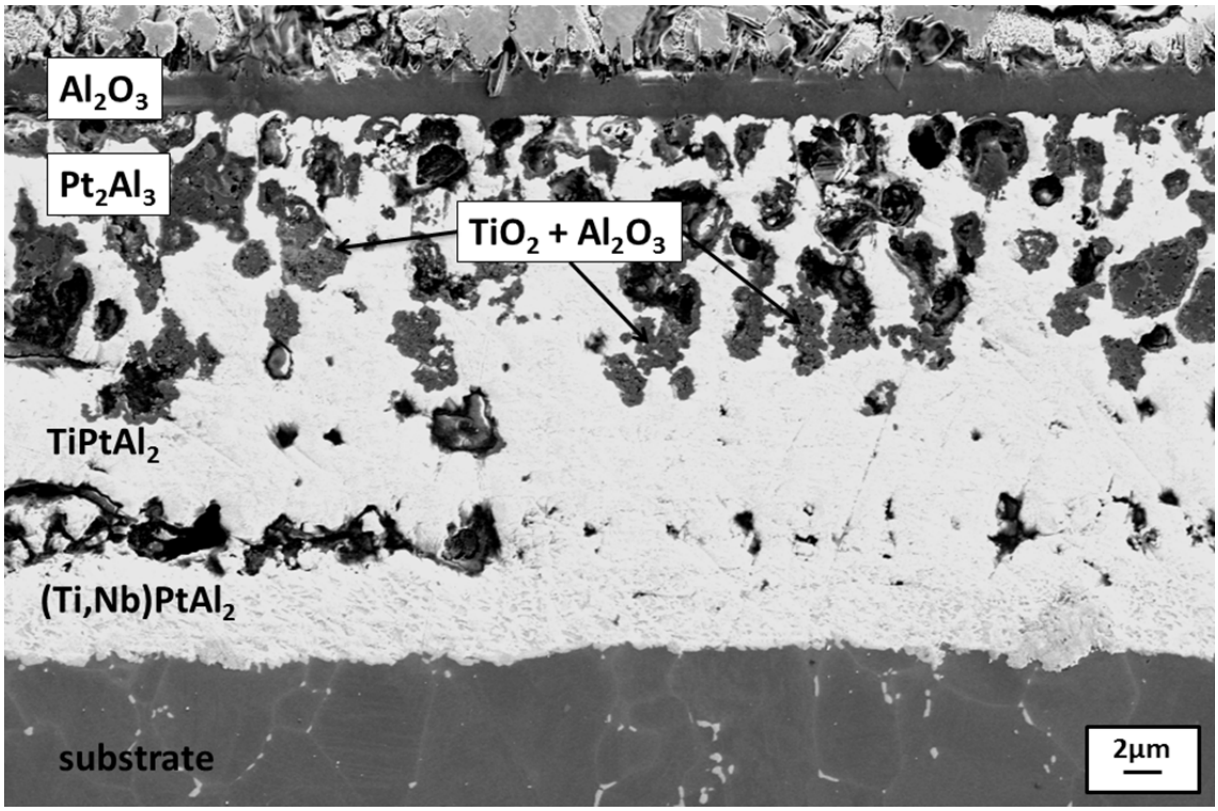

Figure 4c

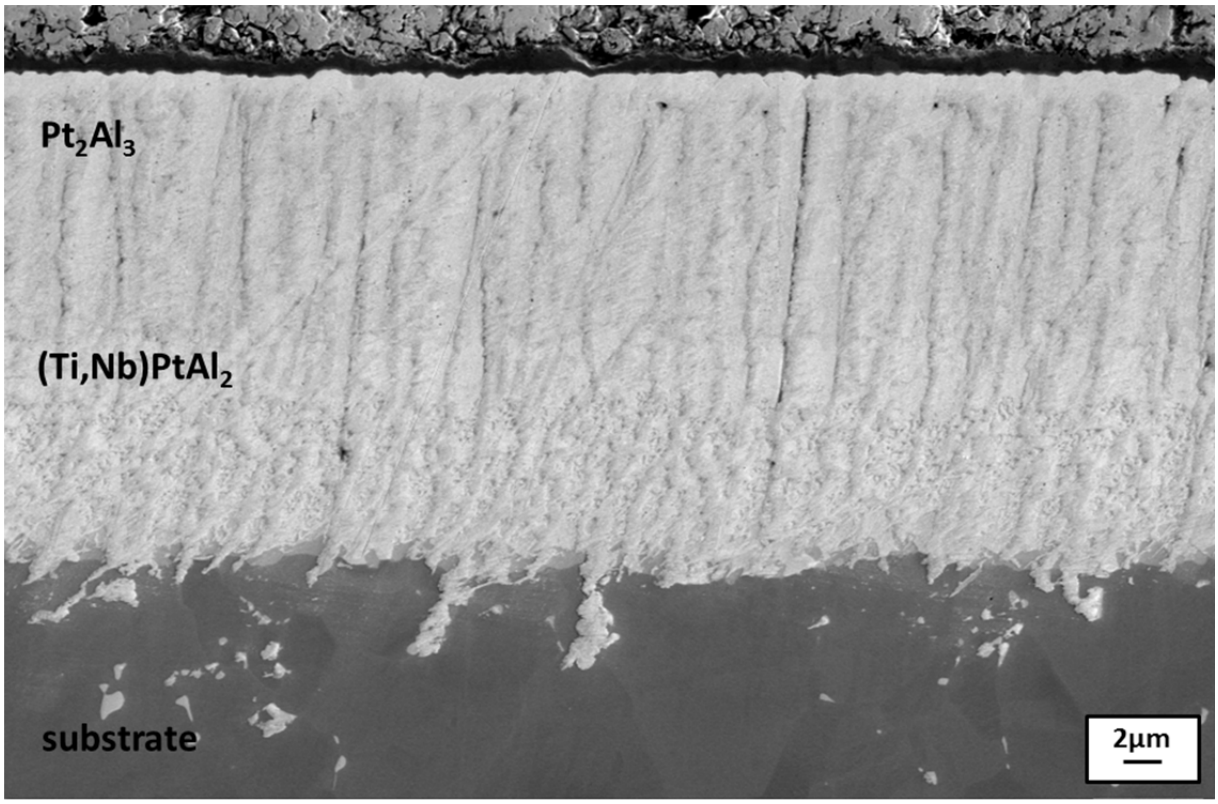

Figure 5a

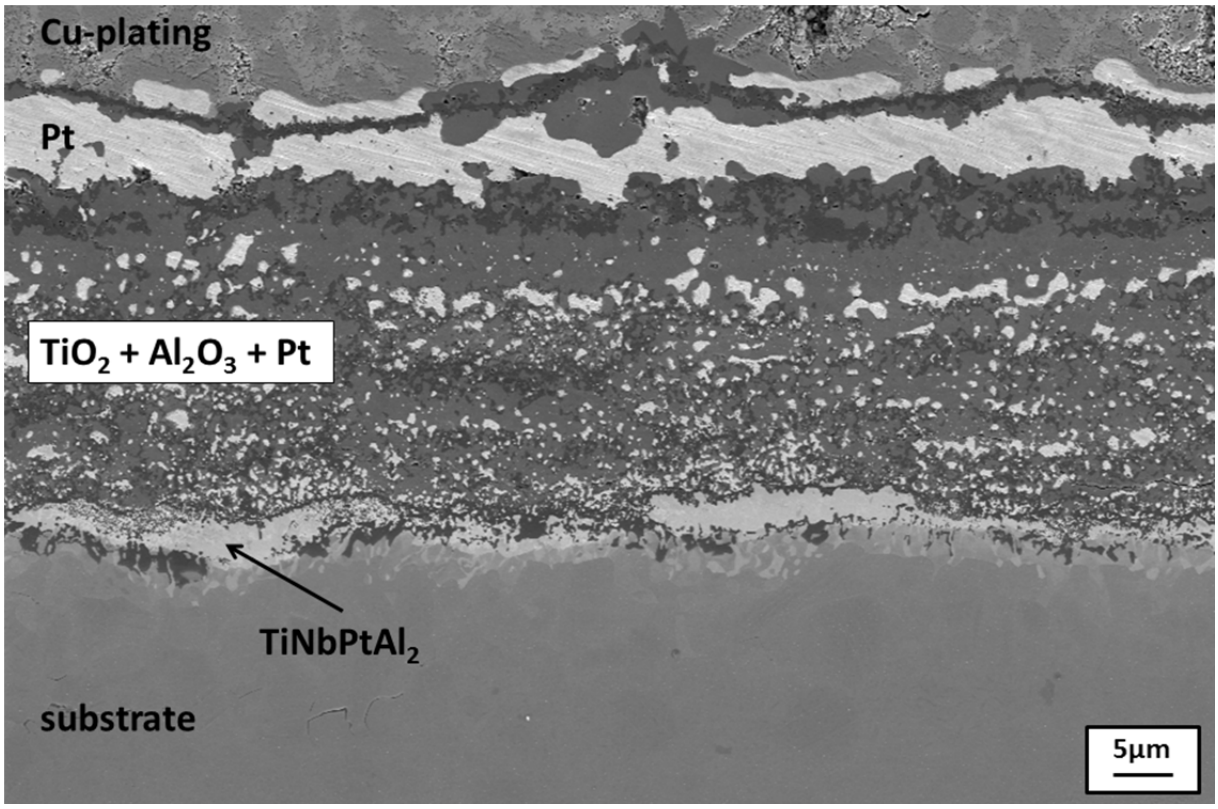

Figure 5b

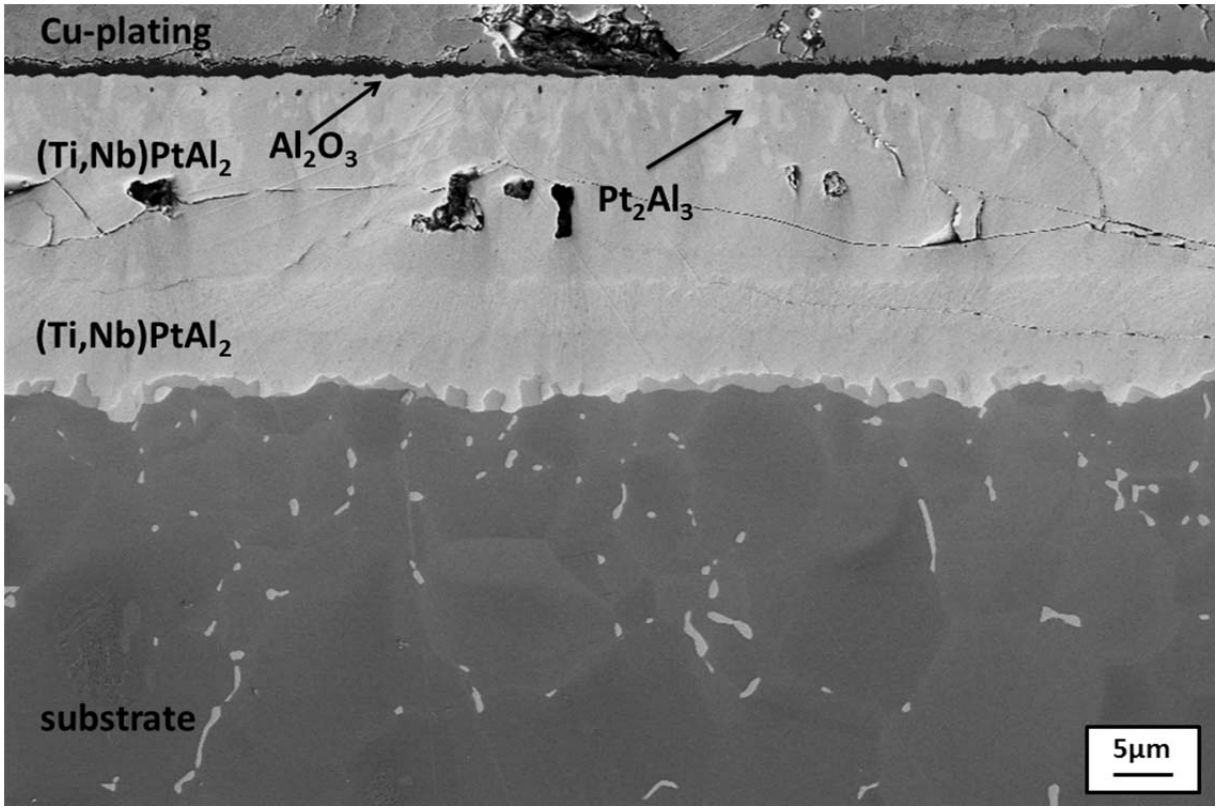

Table 1

Compositions of (Ti,Nb)-Pt-Al phases; measured via EDS

coating	number of test cycles	phase	concentration c [at.%]			
			Al	Ti	Nb	Pt
Pt	10	Ti-Pt-Al	10-30	30-40	2-11	20-50
Pt-53Al	10	Pt_2Al_3	55	2	4	39
		$(Ti,Nb)PtAl_2$	51	17	4	28
		(Ti,Nb)PtAl	30	33	4	33
		$(Ti,Nb)PtAl_2$	45	30	2	23
	100	Pt_2Al_3	54	12	3	31
		$(Ti,Nb)PtAl_2$	50	15	4	29
		$(Ti,Nb)PtAl_2$	37	25	13	25
	1000	Pt_2Al_3	57	13	0	30
		$(Ti,Nb)PtAl_2$	41	32	6	21
Pt-69Al	10	Pt_2Al_3	66	0	0	34
		$(Ti,Nb)PtAl_2$	56	10	5	29
	100	Pt_2Al_3	59	11	0	30
		$TiPtAl_2$	41	38	0	21
		$(Ti,Nb)PtAl_2$	34	42	5	17